

Photoelectrochemical Properties of (In,Ga)N Nanowires for Water Splitting Investigated by in Situ Electrochemical Mass Spectroscopy

Jumpei Kamimura,^{*,†} Peter Bogdanoff,[‡] Jonas Lähnemann,[†] Christian Hauswald,[†] Lutz Geelhaar,[†] Sebastian Fiechter,[‡] and Henning Riechert[†]

[†]Paul-Drude-Institut für Festkörperelektronik, Hausvogteiplatz 5-7, 10117 Berlin, Germany

[‡]Helmholtz-Zentrum Berlin für Materialien und Energie, Glienicker Straße 100, 14109 Berlin, Germany

S Supporting Information

ABSTRACT: We investigated the photoelectrochemical properties of both n- and p-type (In,Ga)N nanowires (NWs) for water splitting by in situ electrochemical mass spectroscopy (EMS). All NWs were prepared by plasma-assisted molecular beam epitaxy. Under illumination, the n-(In,Ga)N NWs exhibited an anodic photocurrent, however, no O₂ but only N₂ evolution was detected by EMS, indicating that the photocurrent was related to photocorrosion rather than water oxidation. In contrast, the p-(In,Ga)N NWs showed a cathodic photocurrent under illumination which was correlated with the evolution of H₂. After photodeposition of Pt on such NWs, the photocurrent density was significantly enhanced to 5 mA/cm² at a potential of -0.5 V/NHE under visible light irradiation of ~40 mW/cm². Also, incident photon-to-current conversion efficiencies of around 40% were obtained at -0.45 V/NHE across the entire visible spectral region. The stability of the NW photocathodes for at least 60 min was verified by EMS. These results suggest that p-(In,Ga)N NWs are a promising basis for solar hydrogen production.

Remarkable results have been achieved in the development of (In,Ga)N alloys as active layer materials of light-emitting and laser diodes.^{1,2} This class of materials is also very promising for solar water splitting because the bandgap can be tuned from the ultraviolet (UV) to the near-infrared region by increasing the indium content, thus covering the entire solar spectrum. In addition, the conduction and valence band edges straddle the H⁺/H₂ and O₂/H₂O redox potentials for In contents (on the group-III sublattice) of up to ~50%, corresponding to a minimum bandgap value of 1.67 eV (equivalent to 740 nm in wavelength).³ However, it is essentially impossible to grow in high structural quality (In,Ga)N layers that are thick enough for efficient light absorption because of the lack of lattice-matched substrates. (In,Ga)N layers have typically been grown on GaN layers. The critical thickness for misfit dislocations, which act as nonradiative recombination centers, is very small (e.g., much <100 nm for 10% In content).⁴ In contrast, nanowires (NWs) are known to accommodate lattice mismatch by lateral elastic relaxation which suppresses the formation of defects.^{5,6} Moreover, the NW geometry offers many other benefits for solar water splitting, such as enhanced light absorption,^{6,7} large surface area for electrochemical reactions,⁷ and improved carrier collection

efficiency.^{7,9} In fact, recently overall water splitting was demonstrated for GaN NW photocatalysts with a noble metal/oxide cocatalyst.¹⁰ However, GaN absorbs only the UV part of the solar spectrum. For (In,Ga)N, there are only very few reports on the photoelectrochemical properties of layers^{11–15} and NWs,¹⁶ and the composition of the gases evolving at the working electrodes was not measured.

Here, we report the investigation of (In,Ga)N NWs for photoassisted water splitting using electrochemical mass spectroscopy (EMS) in a half-cell configuration.^{17,18} This technique enables us to analyze separately the hydrogen evolution reaction (HER) and the oxygen evolution reaction (OER) by detecting volatile products (H₂, O₂, N₂) generated at the working electrode. Our results corroborate the potential of (In,Ga)N NWs for solar hydrogen production and reveal that their stability with respect to photocorrosion depends crucially on the conductivity type.

(In,Ga)N NWs were grown by plasma-assisted molecular beam epitaxy on Si(111) substrates in the self-induced approach.¹⁹ (In,Ga)N grown without any addition of dopants is known to exhibit n-type conductivity, and Mg was used as p-type dopant. Substrates were chosen to exhibit the same type of conductivity as the NWs. The average In content of the (In,Ga)N NWs, measured after growth by X-ray diffraction (XRD) (see Supporting Information, SI), was adjusted from ~4 to 42% by varying the substrate temperature in the range 640–500 °C, thus modifying the In incorporation.^{20,21} The p-doped NWs were grown at 640 °C with Mg cell temperature of 200 °C, corresponding to Mg beam equivalent pressure of 2 × 10⁻¹¹ mbar. More details on the growth are provided as SI. Representative SEM images indicating the morphology of n-In_{0.04}Ga_{0.96}N NWs grown at 640 °C are shown in Figure 1a,b. The NWs were oriented perpendicular to the substrate, and the diameter and height were in the range of 20–200 and 200–400 nm, respectively.

The photoelectrochemical properties were analyzed by EMS. The setup consisted of an electrochemical cell with conventional three-electrode configuration, as shown in Figure 1c. (In,Ga)N NWs on a Si substrate, a platinum wire, a Hg/Hg₂SO₄ electrode, and 0.5 M H₂SO₄ were used as the working, counter, and reference electrodes and electrolyte solution, respectively. The sample (~1 × 1 cm² large) was mounted with resin to the sample

Received: April 23, 2013

Published: June 25, 2013

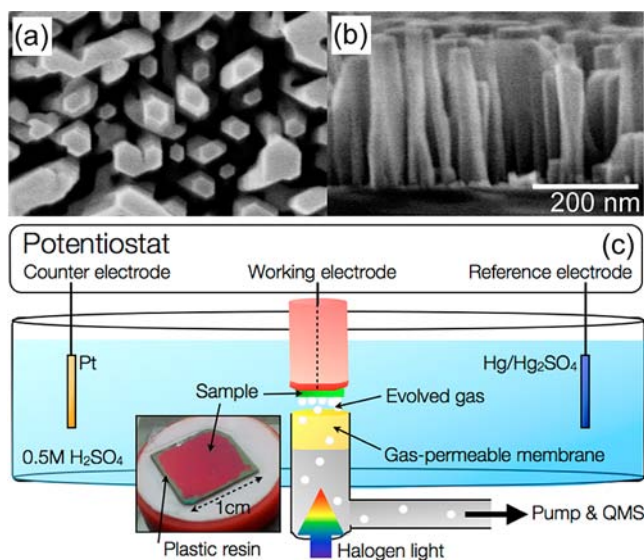


Figure 1. (a) Top view and (b) cross-sectional SEM images of n- $\text{In}_{0.04}\text{Ga}_{0.96}\text{N}$ NWs grown at $640\text{ }^\circ\text{C}$. (c) Schematic image of the photoelectrochemical cell with EMS.

holder, which has a hole in the center in order to contact the sample from the backside without any contact to the electrolyte (Figure 1c). Then the sample (working electrode) was directly attached to the gas-permeable membrane of the inlet system, which was connected to the vacuum system of the quadrupole mass spectrometer (QMS). Volatile products formed at the working electrode during electrochemical experiments can diffuse to some extent through this membrane into the QMS where they are detected simultaneously with the electrochemical data. The sample was illuminated by a halogen lamp through the membrane, and the intensity in front of the sample was $\sim 40\text{ mW/cm}^2$ ($\lambda > 410\text{ nm}$). All measurements were performed in $0.5\text{ M H}_2\text{SO}_4$ at room temperature (RT). Potentials are given with respect to a normal hydrogen electrode (NHE).

To begin with, we focus on the investigation of n-type (In,Ga)N NWs on n-Si(111) substrates. Figure 2 shows as an

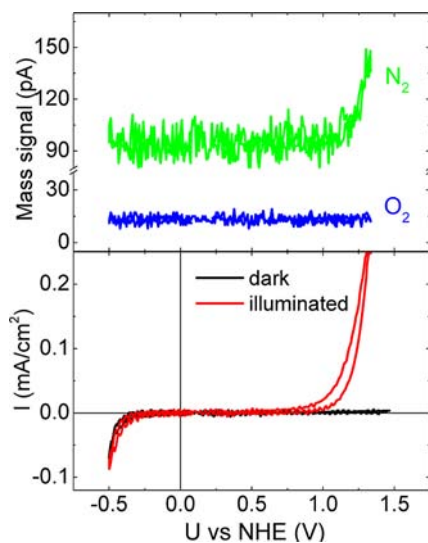


Figure 2. I–V curves (measured first in the dark and then under illumination) and the simultaneously detected mass signals (only under illumination) obtained for n-type $\text{In}_{0.42}\text{Ga}_{0.58}\text{N}$ NWs on n-Si(111).

example the current–voltage (I–V) curves and the corresponding mass signals of N_2 ($m/e = 28$) and O_2 ($m/e = 32$) obtained on n-type $\text{In}_{0.42}\text{Ga}_{0.58}\text{N}$ NWs. In the dark the sample exhibited in the forward direction a cathodic current at potentials more negative than -0.25 V/NHE . This current was attributed to the H_2 evolution reaction (mass signal not shown). In the reverse direction no noteworthy current was detected up to 1.5 V/NHE , as it is expected for n-type material. Under illumination, no significant change was observed in the forward direction, whereas in the reverse direction a positive (anodic) light-induced current was now measured starting at a potential of $\sim 0.75\text{ V/NHE}$. However, instead of O_2 , only a N_2 mass signal was detected, and the slope and onset potential of this signal correlated well with those of the photocurrent. These results indicate that instead of water oxidation a corrosion process took place, and the evolution of N_2 resulted from the decomposition of (In,Ga)N. The illumination only seems to induce photoconductivity in the material which enables the corrosion process at low bias. We carried out similar experiments with other samples, and all investigated n-type (In,Ga)N NWs suffered from photo-corrosion, while no water oxidation was observed. These measurements highlight the importance of in situ EMS, because acquiring only I–V curves may lead to a wrong interpretation.

Now we turn to the photoelectrochemical properties of p-type (In,Ga)N NWs on p-Si(111) and the HER that is expected for such samples. Figure 3 presents the I–V curves in the dark and

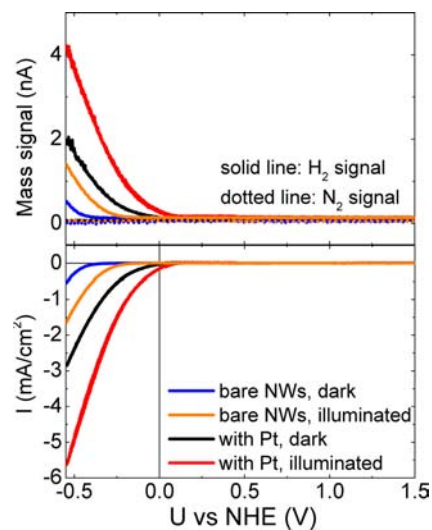


Figure 3. I–V curves (measured first in the dark and then under illumination) and the corresponding mass signals (solid lines for H_2 , dotted lines for N_2) for p- $\text{In}_{0.04}\text{Ga}_{0.96}\text{N}$ NWs on p-Si substrate without and with Pt cocatalysts.

under illumination and the corresponding mass signals of H_2 and N_2 for Mg-doped $\text{In}_{0.04}\text{Ga}_{0.96}\text{N}$ NWs (blue and orange lines). In the reverse direction a small cathodic current was measured in the dark for potentials more negative than -0.3 V/NHE . Under illumination, the absolute current was increased, and the onset was shifted by $\sim 200\text{ mV}$ to positive potential. This change in current with illumination is consistent with the expected p-type conductivity. The type of conductivity is corroborated by two additional observations: First, open circuit potential measurements in the dark and under illumination indicated a positive photoinduced voltage shift of $\sim 200\text{ mV}$. Second, both in the dark and under illumination no significant current was detected in the forward direction up to 1.5 V/NHE . As seen in Figure 3, the

photocurrent in the reverse direction coincided with the evolution of H_2 . In order to unambiguously assign both the photocurrent and the generation of H_2 to the NWs, we carried out equivalent experiments using a p-type Si substrate without NWs and found only a very small photocurrent and no gas detection (see Figure S2). Finally, Figure 3 shows that during the measurements with NWs, the N_2 signal remained at the noise level. Similar results for all these types of experiments were obtained for other samples with p-type (In,Ga)N NWs. Therefore, this type of NW does not suffer from photocorrosion, and the photocurrent is involved in the HER.

In order to clarify whether the kinetics of the electrochemical reaction limit the overall photocurrent, we deposited platinum onto the (In,Ga)N NWs as a cocatalyst (see SI), which is known to be the best cocatalyst for the HER in acidic solutions.²² Figure 3 contains additional I–V curves measured in the dark and under illumination on Pt-decorated p-In_{0.04}Ga_{0.96}N NWs on p-Si substrate (black and red lines). Compared to the bare p-(In,Ga)N NWs, the modification with platinum leads to a significant increase of both dark and photocurrent. Thus, the overall photocurrent is limited by the electrochemical kinetics of the HER and not by the generation of charge carriers or their migration to the electrode interface. In particular, for the platinum-modified sample the onset of the photocurrent is shifted by ~ 400 mV to positive potentials. Moreover, the QMS signal reveals that the photocurrent is attributed to the H_2 evolution even at potentials positive compared to 0 V/NHE, i.e., the redox potential of the HER. This observation clearly proves the generation of a photovoltage in the p-(In,Ga)N NWs which assists the HER. Again, we excluded any possible effect of the p-Si substrate by performing equivalent experiments with Pt-modified Si substrates bare of NWs (see Figure S2). These results unambiguously demonstrate that p-(In,Ga)N NWs are under our experimental conditions active in the photoelectrochemical HER.

The dark current density of the p-(In,Ga)N NWs was relatively high, and it was increased further by the Pt modification. These observations suggest the presence of recombination centers in the bulk and at the electrode/electrolyte interface, which can be explained by structural defects. We believe that the photocurrent and the photovoltage could be improved further if a way was found to reduce the concentration of these defects. Additional enhancements could be achieved by the optimization of the platinum photodeposition in terms of particle size and dispersion. This work is in progress and will be published in a forthcoming paper.

The obtained values for the photocurrents are already fairly remarkable for the present samples. Under an illumination intensity < 40 mW/cm², a photocurrent density of 5 mA/cm² at -0.5 V/NHE was observed. These values are significantly higher than those of p-In_{0.12}Ga_{0.88}N films which exhibited only 0.3 mA/cm² at -1.9 V/NHE under 405 nm illumination with 30 mW/cm².¹⁵ This comparison is consistent with the expected benefits of the NW geometry compared to planar films.

In order to assess the photoelectrochemical properties of the p-type (In,Ga)N NWs in more detail, we measured the incident photon-to-current conversion efficiency (IPCE, see SI). Figure 4a shows the respective data acquired for the same sample at a bias potential of -0.45 V/NHE with monochromatic light using various band-pass filters with 15–30 nm full width at half-maximum. High IPCE values of around 40% were observed across the entire visible wavelength range. Although this experiment was performed under bias condition, the results

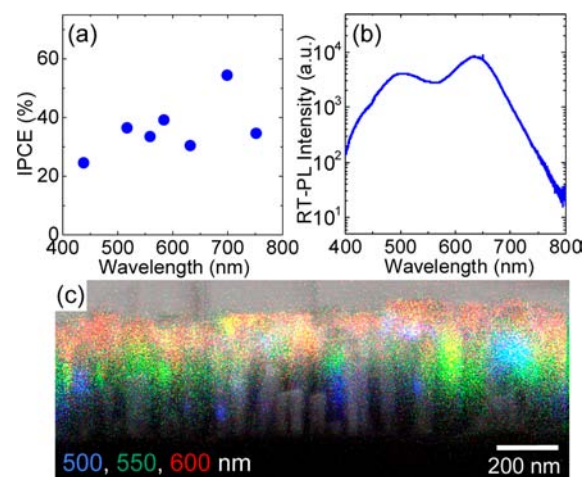


Figure 4. (a) IPCE of Pt-covered p-In_{0.04}Ga_{0.96}N NWs as a function of the wavelength of the incident light, measured at a potential of -0.45 V/NHE. (b) RT photoluminescence spectrum of such NWs. (c) False-color cathodoluminescence mapping superimposed on the corresponding cross-sectional SEM image of such NWs. Emission at 500, 550, and 600 nm is depicted in blue, green, and red, respectively.

demonstrate the high efficiency of light absorption in (In,Ga)N NWs for a wide spectral range, which in turn indicates excellent prospects for solar water splitting.

Very interestingly, the average In concentration of these p-(In,Ga)N NWs as determined by XRD was only $\sim 4\%$, which corresponds to a band gap of 3.25 eV (381 nm) using a bowing parameter of 1.43.²³ Thus, the high IPCE values obtained for longer wavelengths cannot be explained under the assumption of a homogeneous distribution of In in the NWs. Indeed, the RT photoluminescence spectrum of this sample presented in Figure 4b also shows very broad emission covering the whole visible spectrum (experimental details in SI). For that reason a cathodoluminescence mapping was performed (see Figure 4c) revealing that different regions within the NW ensemble and within single NWs emit light of different color. Hence, there are compositional fluctuations along individual NWs and between different NWs, consistent with observations by others.²⁴ For a detailed explanation of the growth processes and the optoelectronic properties of the NWs, further experiments have to be performed. However, it is well-known that variations in In content are very common for (In,Ga)N alloys, in general,²⁵ and can be both beneficial²⁶ and detrimental.²⁷ In this study, the compositional fluctuations seem to extend the spectral range for efficient absorption and to increase the photocurrent. As a matter of fact, the longest wavelength for which we measured the ICPE was 750 nm. The equivalent band gap energy corresponds fairly well to the maximum In content of 50% for which solar water splitting with (In,Ga)N is expected. In view of the large compositional fluctuations found in the NWs of the present study, future research is needed to elucidate the precise correlation between In content, light absorption, and hydrogen generation.

In order to assess the long-term stability of the p-(In,Ga)N NWs under HER conditions, we carried out potentiostatic EMS experiments as shown in Figure 5. First, the background signal was detected for 10 min without any bias potential or illumination. Then, the sample was biased at -0.45 V/NHE in the dark for 10 min. The value of the observed dark current agrees well with the dark current seen in Figure 3 and did not change significantly over 10 min. At the same time, some

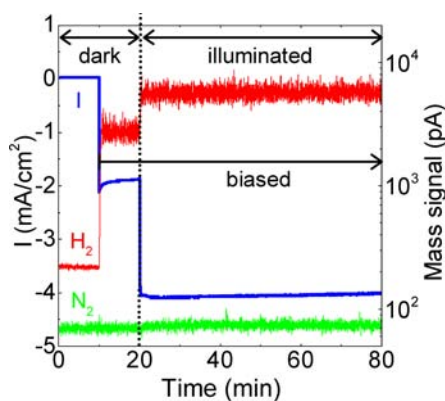


Figure 5. Stability of the cathodic current and the corresponding mass signals of H_2 and N_2 obtained for Pt-covered p- $\text{In}_{0.04}\text{Ga}_{0.96}\text{N}$ NWs. After 10 min, the sample was biased at -0.45 V/NHE, and after additional 10 min it was irradiated with visible light.

hydrogen evolved, also in accord with the data in Figure 3. Finally, the sample was illuminated, and both the current and the H_2 signal increased instantaneously. Very importantly, both values were stable for at least 60 min, and no N_2 was detected. Therefore, in contrast to n-type (In,Ga)N NWs, p-(In,Ga)N NW are stable under electrochemical conditions and sustain the HER.

In summary, the simultaneous acquisition of I - V curves in an electrochemical cell and in situ detection of the evolved gases by EMS showed that n-type (In,Ga)N NWs are prone to suffer from photocorrosion. In contrast, for p-type (In,Ga)N NWs we measured a cathodic photocurrent under illumination and observed the evolution of H_2 , thus corroborating the principal suitability of these NWs for solar water splitting. After Pt was deposited on such NWs, we obtained a high current density of 5 mA/cm^2 at a potential of -0.5 V/NHE, although the light intensity was <40 mW/cm^2 . Moreover, the IPCE was around 40% in the entire visible wavelength region, and both photocurrent and hydrogen evolution were stable for at least 60 min, indicating the excellent potential of these NWs for solar water splitting. This study is the first demonstration of solar hydrogen evolution using (In,Ga)N NWs by the detection of the evolved gases and thus paves the way for the development of a new class of photoelectrodes.

■ ASSOCIATED CONTENT

📄 Supporting Information

Experimental details and additional results. This material is available free of charge via the Internet at <http://pubs.acs.org>.

■ AUTHOR INFORMATION

Corresponding Author

kamimura@pdi-berlin.de

Notes

The authors declare no competing financial interest.

■ ACKNOWLEDGMENTS

The authors thank A.-K. Bluhm for SEM support, C. Herrmann as well as H.-P. Schönherr for the maintenance of the MBE system, W. Anders and B. Drescher for backside metallization, D. Stellmach for help with photoelectrochemical measurements, and U. Jahn and R. van de Krol for a critical reading of the manuscript. J.K. is grateful to Leibniz Association and German

Academic Exchange Service (DAAD) for a Leibniz-DAAD postdoctoral fellowship.

■ REFERENCES

- (1) Ponce, F. A.; Bour, D. P. *Nature* **1997**, *386*, 351–359.
- (2) Nakamura, S.; Senoh, M.; Nagahama, S.; Iwasa, N.; Yamada, T.; Matsushita, T.; Kiyoku, H.; Sugimoto, Y. *Jpn. J. Appl. Phys.* **1996**, *35*, L74–L76.
- (3) Moses, P. G.; Van de Walle, C. G. *Appl. Phys. Lett.* **2010**, *96*, 021908–1–021908–3.
- (4) Holec, D.; Costa, P. M. F. J.; Humphreys, C. J. *J. Cryst. Growth* **2007**, *303*, 314–317.
- (5) Ertekin, E.; Greaney, P. A.; Chrzan, D. C.; Sands, T. D. *J. Appl. Phys.* **2005**, *97*, 114325–1–114325–10.
- (6) Glas, F. *Phys. Rev. B* **2006**, *74*, 121302–1–121302–4.
- (7) Hiralal, P.; Unalan, H.; Amaratunga, G. *Nanotechnology* **2012**, *23*, 194002–1–194002–17.
- (8) Kelzenberg, M. D.; Boettcher, S. W.; Petykiewicz, J. A.; Turner-Evans, D. B.; Putnam, M. C.; Warren, E. L.; Spurgeon, J. M.; Briggs, R. M.; Lewis, N. S.; Atwater, H. A. *Nat. Mater.* **2010**, *9*, 239–244.
- (9) Kayes, B. M.; Atwater, H. A.; Lewis, N. S. *J. Appl. Phys.* **2005**, *97*, 114302–1–114302–11.
- (10) Wang, D.; Pierre, A.; Kibria, M. G.; Cui, K.; Han, X.; Bevan, K. H.; Guo, H.; Paradis, S.; Hakima, A. R.; Mi, Z. *Nano Lett.* **2011**, *11*, 2353–2357.
- (11) Fujii, K.; Kusakabe, K.; Ohkawa, K. *Jpn. J. Appl. Phys., Part 1* **2005**, *44*, 7433–7435.
- (12) Li, J.; Lin, J. Y.; Jiang, H. X. *Appl. Phys. Lett.* **2008**, *93*, 162107–1–162107–3.
- (13) Aryal, K.; Pantha, B. N.; Li, J.; Lin, J. Y.; Jiang, H. X. *Appl. Phys. Lett.* **2010**, *96*, 052110–1–052110–3.
- (14) Mauder, C.; Tuna, Ö.; Gutrath, B.; Balmes, V.; Behmenburg, H.; Rzhetskii, M. V.; Lutsenko, E. V.; Yablonskii, G. P.; Noyong, M.; Simon, U.; Heuken, M.; Kalisch, H.; Vescan, A. *Phys. Stat. Sol. C* **2012**, *9*, 964–967.
- (15) Usui, S.; Kikawa, S.; Kobayashi, N.; Yamamoto, J.; Ban, Y.; Matsumoto, K. *Jpn. J. Appl. Phys.* **2008**, *47*, 8793–8795.
- (16) Hwang, Y.; Wu, C. H.; Hahn, C.; Jeong, H. E.; Yang, P. *Nano Lett.* **2012**, *12*, 1678–1682.
- (17) Bogdanoff, P.; Alonso-Vante, N. *Ber. Bunsenges Phys. Chem.* **1993**, *97*, 940–943.
- (18) Bogdanoff, P.; Friebe, P.; Alonso-Vante, P. *J. Electrochem. Soc.* **1998**, *145*, 576–582.
- (19) Geelhaar, L.; Chèze, C.; Jenichen, B.; Brandt, O.; Pfüller, C.; Münch, S.; Rothemund, R.; Reitzenstein, S.; Forchel, A.; Kehagias, T.; Kominou, P.; Dimitrakopoulos, G. P.; Karakostas, T.; Lari, L.; Chalker, P. R.; Gass, M. H.; Riechert, H. *IEEE J. Sel. Top. Quantum Electron.* **2011**, *17*, 878–888.
- (20) Calleja, E.; Ristić, J.; Fernández-Garrido, S.; Cerutti, L.; Sánchez-García, M. A.; Grandal, J.; Trampert, A.; Jahn, U.; Sánchez, G.; Griol, A.; Sánchez, B. *Phys. Status Solidi B* **2007**, *244*, 2816–2837.
- (21) Wölz, M.; Fernández-Garrido, S.; Hauswald, C.; Brandt, O.; Limbach, F.; Geelhaar, L.; Riechert, H. *Cryst. Growth Des.* **2012**, *12*, 5686–5692.
- (22) Walter, M. G.; Warren, E. L.; Boettcher, S. W.; Mi, Q.; McKone, J. R.; Santori, E. A.; Lewis, N. S. *Chem. Rev.* **2010**, *110*, 6446–6473a.
- (23) Wu, J.; Walukiewicz, W.; Yu, K. M.; Ager, J. W., III; Haller, E. E.; Lu, H.; Schaff, J. *Appl. Phys. Lett.* **2002**, *80*, 4741–4743.
- (24) Goodman, K. D.; Protasenko, V. V.; Verma, J.; Kosel, T. H.; Xing, H. G.; Jena, D. *J. Appl. Phys.* **2011**, *109*, 084336–1–084336–10.
- (25) Ho, I.; Stringfellow, G. B. *Appl. Phys. Lett.* **1996**, *69*, 2701–2703.
- (26) Chichibu, S. F.; Uedono, A.; Onuma, T.; Haskell, B. A.; Chakraborty, A.; Koyama, T.; Fini, P. T.; Keller, S.; Denbaars, S. P.; Speck, J. S.; Mishra, U. K.; Nakamura, S.; Yamaguchi, S.; Kamiyama, S.; Amano, H.; Akasaki, I.; Han, J.; Sota, T. *Nat. Mater.* **2006**, *5*, 810–816.
- (27) Sizov, D.; Bhat, R.; Zah, C.-E. *J. Lightwave Technol.* **2012**, *30*, 679–699.